

FILE COPY
No. 1

FILE COPY
To be returned to the Files of
Ames Aeronautical Laboratory
National Advisory Committee
for Aeronautics
Moffett Field, Calif.

~~100~~
100

TECHNICAL NOTES

NATIONAL ADVISORY COMMITTEE FOR AERONAUTICS

No. 713

A COMPARISON OF SEVERAL TAPERED WINGS
DESIGNED TO AVOID TIP STALLING
By Raymond F. Anderson
Langley Memorial Aeronautical Laboratory

A 06
9871
100

Washington
June 1939

NATIONAL ADVISORY COMMITTEE FOR AERONAUTICS

TECHNICAL NOTE NO. 713

A COMPARISON OF SEVERAL TAPERED WINGS

DESIGNED TO AVOID TIP STALLING

By Raymond F. Anderson

SUMMARY

Optimum proportions of tapered wings were investigated by a method that involved a comparison of wings designed to be aerodynamically equal. The conditions of aerodynamic equality were equality in stalling speed, in induced drag at a low speed, and in the total drag at cruising speed. After the wings were adjusted to aerodynamic equivalence, the weights of the wings were calculated as a convenient method of indicating the optimum wing. The aerodynamic characteristics were calculated from wing theory and test data for the airfoil sections. Various combinations of washout, camber increase in the airfoil sections from the center to the tips, and sharp leading edges at the center were used to bring about the desired equivalence of maximum lift and center-stalling characteristics.

In the calculation of the weights of the wings, a simple type of spar structure was assumed that permitted an integration across the span to determine the web and the flange weights. The covering and the remaining weight were taken in proportion to the wing area. The total weights showed the wings with camber and washout to have the lowest weights and indicated the minimum for wings with a taper ratio between $1/2$ and $1/3$.

INTRODUCTION

Many investigations have been made of the aerodynamic and the structural aspects of tapered wings with a view to finding the best taper ratio. Investigations of taper ratio are reported in references 1 and 2. A general discussion of tapered wings is given in reference 3. Although

drag and weight were considered in references 1 and 2, the effect of taper ratio on the maximum lift and the manner of stalling of wings was not considered. The effect of taper ratio on the maximum lift is considerable. The tip stall that usually results from the use of tapered wings, moreover, evidences itself as instability in roll at angles of attack less than that corresponding to the maximum lift coefficient. This condition is generally recognized as undesirable from the point of view of handling characteristics in low-speed flight.

It is accordingly considered herein that wings should be designed to avoid tip stalling. With this point of view, wings of different taper ratio were designed to be aerodynamically equal; that is, equal in stalling speed, in induced drag at a low speed, and in total drag at cruising speed. The weights were then calculated to indicate the "optimum" wing (the wing of lowest weight).

In the calculation of the maximum lift, the areas were so obtained that they approximate the values which would be required by wings with full-span flaps. The effect of partial-span flaps was not considered.

Wings with taper ratios of $1/2$, $1/3$, and $1/4$ were considered for a large airplane. In the determination of the maximum lift coefficients, a margin against the stalling of the tips was specified. For the three taper ratios the stalling of three sets of wings was considered: wings with no washout or camber increase in the airfoil sections from center to tip (referred to as the "basic" series, to be described later); wings with washout; and wings with washout and camber increase from center to tips. For each of the three sets of wings, lift-spoiling devices, such as sharp leading edges, were assumed at the center of the wings to make up the required balance of the margin against stalling of the tips. This procedure is practically equivalent to increasing the lift by the use of leading-edge slots over all of the span except for a small portion of the center. The comparative effects of washout and camber should therefore be nearly independent of whether the lift is decreased at the center or increased at the tips.

ASSUMPTION FOR THE AERODYNAMIC CALCULATIONS

The wings had straight tapers and rounded tips and were of a size suitable for a four-engine airplane of 64,000 pounds gross weight with a wing loading of approximately 30 pounds per square foot. The tip chord of the trapezoid enclosing the rounded tips was used to define the taper ratio, as in reference 4. The distribution of thickness along the span and of camber and washout, when they were used, was linear. A thickness ratio of 0.09 was taken for the airfoil sections at the tips. A basic wing, used to determine the aerodynamic values to be equaled by the other wings, had a root thickness ratio of 0.14, an area of 2,200 square feet, a taper ratio of $1/3$, and a span of 138.2 feet. The method of calculating the dimensions of the other wings will be given later. The symbols used are listed in an appendix.

Prevention of Tip Stalling

For the first series of wings of varying taper ratio, the method for prevention of tip stalling was the use of sharp leading edges to reduce $c_{l_{max}}$ at the center of the wings. This series of wings was called the basic series because it included the basic wing of taper ratio $1/3$ used to establish the aerodynamic values. The N.A.C.A. 230 series airfoil sections listed in table I were used.

For a second series of wings, washout was used; and, for the third series, washout was combined with an increase in camber of the airfoil sections from center to tips. The increase in camber produces an increase in the $c_{l_{max}}$ of the sections near the tips and thereby causes the stalling point to move inward. For the wings with washout, small amounts of washout were used to prevent excessive increase in the induced drag. Sharp leading edges at the center of the wings were then used to make up the balance of the margin required against stalling of the tips. The case of taper ratio $1/4$ was omitted for the series with washout alone because too thin a wing would have resulted.

For all the wings, in order to insure the avoidance of tip stalling, a certain c_l margin was specified at $0.7 b/2$ when $C_{L_{max}}$ was reached. (See fig. 1.) The mar-

gin required depended on the calculated spanwise position of the stalling point without sharp leading edges. This point occurred where a c_l curve corresponding to the spanwise load distribution became tangent to the $c_{l_{max}}$ curve, as outlined in detail in reference 4. When this stalling point was at or inside $0.7 b/2$, the c_l margin at $0.7 b/2$ was taken as 0.1. When it was outside $0.7 b/2$, the margin was increased in the ratio of the distance from the center of the wing to $0.7 b/2$. The provision of this amount of margin when stalling started at the center gave a calculated positive damping in roll at the stall that should prevent sudden dropping of a wing.

Conditions of Aerodynamic Equality

For the first of the conditions of aerodynamic equality, equal stalling speeds, plain airfoil sections were assumed when $C_{L_{max}}$ was computed because of the availability of the $c_{l_{max}}$ data. The Reynolds Number at stalling speed was made to fall within the usual range for an airplane of the size assumed by basing it on the stalling speed with flaps, so that the wings had approximately the same areas as wings with full-span flaps. That the condition of stalling-speed equality would not be appreciably altered by considering the wings to have full-span flaps was verified from figure 60 of reference 5, which gives the $c_{l_{max}}$ increments produced by flaps. (The range of the average thickness of the wings was small.)

As the stalling speed V_S is equal to $\sqrt{\frac{2W_g}{\rho S C_{L_{max}}}}$ and W_g was fixed, the stalling-speed condition required that the product $SC_{L_{max}}$ for each wing be equal to the product for the basic wing (taper ratio 1/3).

The second condition was that the induced drags should be equal at a speed corresponding to a C_L of 1.0 for the basic wing (low-speed condition). The induced drag rather than the total drag was used because the induced drag was nearly all of the drag and was relatively easy to calculate. The induced drag, with the effect of twist ϵ included, may be found from

$$D_i = \frac{W_g^2}{q \pi b^2 u} + W_g \epsilon a_0 v + q S (\epsilon a_0)^2 w \quad (1)$$

or the spans required to make the induced drags equal may be expressed

$$\frac{b}{b_b} = \sqrt{\frac{u_b D_{i_b}}{u [D_{i_b} - W_g \epsilon a_0 v - q S (\epsilon a_0)^2 w]}} \quad (2)$$

where the subscript b refers to the basic wing, and

$$D_{i_b} = \frac{W_g^2}{q \pi b_b^2 u_b} \quad (3)$$

Equation (3) is equation (1) with the last two terms omitted because the basic wing has no twist. These equations were derived from the formula for C_{D_i} given in reference 4.

The third condition, equal cruising speeds, was satisfied by making the drags equal at cruising speed, as the power was assumed constant. Cruising speed corresponded to a C_L of 0.3 for the basic wing.

METHOD OF CALCULATION

Proportions and Aerodynamic Characteristics

The method used for calculating $C_{L_{max}}$, C_{D_0} , and the other aerodynamic characteristics of the wings has been found to give results that agree well with test results (references 4 and 6).

The method of calculating the maximum lift coefficient for the basic wing is illustrated in figure 1. For this wing, $c_l = c_{l_a}$ because there is no washout and therefore $c_{l_b} = 0$. Stalling was calculated to occur without any sharp leading edge at $0.7 b/2$; that is, c_{l_a} would reach $c_{l_{max}}$ first at the 0.7 point. (See reference 4 for a detailed

explanation.) A value of c_{l_a} of 0.1 less than the $c_{l_{max}}$ at $y = 0.7 b/2$ (c_{l_a}') was then the lift coefficient corresponding to C_{Lmax} . Numerically, $C_{Lmax} = c_{l_a}' / c_{l_{a1}}$, where $c_{l_{a1}}$ was taken at $y = 0.7 b/2$. The values of $c_{l_{max}}$ at the center of the wing were then considered to be reduced by a sharp leading edge to the values of c_{l_a} , as shown, so that stalling would begin at the center of the wing. The values of $c_{l_{max}}$ used for calculating C_{Lmax} for this wing were taken from reference 5.

The value of the induced drag at the low-speed condition for the basic wing, D_{i_b} , to be used in finding the spans of the other wings was calculated from equation (3).

The drag of the basic wing at cruising speed was calculated in terms of q in the form

$$\frac{D}{q} = \frac{D_o}{q} + \frac{D_i}{q} \quad (4)$$

The value of D_o/q was calculated for a C_L of 0.3 and for the cruising-speed Reynolds Number (as outlined in reference 4) by a graphical integration along the span of the section drags from

$$\frac{D_o}{q} = \int_0^{b/2} c_{d_o} c \, dy \quad (5)$$

The values of c_{d_o} were taken from reference 7 for the basic wing as well as for the others. The value of D_i/q was calculated from equation (3) for a value of q corresponding to the cruising speed.

With the values for the basic wing established, equal values for the other wings were found by successive approximations. For the other two wings of the basic series, a root thickness and an area were assumed that, it was hoped, would produce the desired characteristics. An approximate

span was then found from equation (2) so that c and c_{t_a} could be found. For these values, $C_{L_{max}}$ was then calculated in the same manner as for the basic wing.

For the wings with washout and with washout and camber increase, airfoil sections and washout were assumed. The value of $C_{L_{max}}$ was then calculated as for the basic wing, except that c_{t_b} due to washout was combined with c_{t_a} to obtain c_t , as shown in figure 2.

From the values of $C_{L_{max}}$ for the wings, a more accurate value of S was found for each wing to obtain a product of S and $C_{L_{max}}$ equal to the value for the basic wing. The approximate span was used to calculate the aspect ratio so that the induced-drag factors u , v , and w could be found from reference 4. A more accurate value of the span to obtain the required induced drag at low speed could then be found from equation (2). A value of a_0 of 0.1 per degree was used. From S and b , more accurate values of c could be found so that D/q could be computed.

The value of D/q at cruising speed for each wing was next found from equation (4), where the value of D_0/q was calculated from equation (5) for a C_L corresponding to the cruising speed and the wing area. The value of D_i/q was then found from equation (1) for a value of q corresponding to the cruising speed. If the values of D/q calculated in this manner were not close to the value for the basic wing, new values of root thickness ratio were assumed and the calculations were repeated.

Successive approximations were repeated in this manner until the required values of $SC_{L_{max}}$, b , and D/q were obtained. Two or three approximations were usually required. The resulting dimensions and the values of D/q are given in table I. The amounts of washout required were a compromise between a high $C_{L_{max}}$ and a low induced drag. In order to investigate the effect of greater washout, calculations were made for a wing with camber increase and washout with a taper ratio of 1/3, and with $\epsilon = -4^\circ$, but the results were not included in the table because the weight was excessively increased. It should be noted that

the washout is "aerodynamic"; that is, it is measured, not from the chord, but from the zero-lift directions of the root and the tip sections.

Weight of the Wings

The load factors for calculating the weights of the wings were computed as specified in reference 8. A high speed of 240 miles per hour was used with a gust of 30 feet per second, as given for condition I in reference 8. The lift-curve slope was computed from figure 2 of reference 4. The values of the limit-load factors n , computed in this manner, are listed in table I.

The C_N to be used for calculating the load on the wings was then found from

$$C_N = \frac{n(W_g - W)}{qS} \quad (6)$$

where W_g is the gross weight; W , the assumed wing weight; and q corresponds to a speed of 240 miles per hour. The load distribution per unit length along the span, l , was then found from $l = q c_l c$ where c_l was found as in reference 4 from

$$c_l = C_N c_{l_{a1}} + c_{l_b} \quad (7)$$

For the wings without twist, c_{l_b} is zero.

The values of $c_{l_{a1}}$ and c_{l_b} were calculated from the load-distribution data given in reference 4 so that the variation of the load distribution with taper was taken into account. From the distribution of load across the span, the distribution of the shear and the moment could be easily found.

The shears and the moments were assumed to be carried by a single spar with a simple type of structure as shown in figure 3, so that the weights of the material could be

found by an integration across the span. The torsion load not eliminated by assuming the spar to be located at the lift center of each section may be considered to be carried by the skin.

The relieving loads caused by the engines and the fuselage were taken into account so that the total wing weights were calculated in the form

$$W = W_W - \Delta W_W + W_F - \Delta W_F + W_C \quad (8)$$

The weights thus calculated may not agree with the weights of actual airplane wings because of the simple type of structure assumed and the improbability that all the material will develop the stress assumed. The effects of the assumptions should, however, be similar on all the wings so that the correct relative weights should be obtainable.

The load distributions across the semispan of the wings, computed in the manner previously given, had the form represented in figure 3. From the load, or $c_l c$, curves, the shears and the moments at any point y along the semispan were found from

$$F_S = q \int_y^{b/2} c_l c \, dy \quad (9)$$

$$M = \int_y^{b/2} F_S \, dy \quad (10)$$

The shear bracing was assumed to have an angle of 45° , as shown in figure 3. For a unit length along the span dy corresponding to a unit length of bracing dL , the weight of the web will be

$$dW_W = p \frac{f}{s} dL = p \frac{F_S}{0.707s} \frac{dy}{0.707} = \frac{2p F_S}{s} dy \quad (11)$$

where

10

N.A.C.A. Technical Note No. 713

p is the specific weight (assumed to be an aluminum alloy weighing 0.1 pound per cubic inch).

s , allowable stress.

f , force in a diagonal.

For a factor of safety of 1.5, the web weight for both halves of the wing is then

$$W_W = 4 \times 1.5 \frac{p}{s} \int_0^{b/2} F_S dy \quad (12)$$

A conservative stress of 20,000 pounds per square inch was assumed in calculating W_W .

In the calculation of the weight of the flanges, the moment at any point along the span was considered to be carried by tension and compression in the flanges. If F is the force in a flange (fig. 3) and if the effective thickness of the beam t' is taken as 0.9 the wing thickness, then the weight of a unit length of one flange will be

$$dW_F = p \frac{F}{s} dy = p \frac{M}{t' s} dy \quad (13)$$

The weight of upper and lower flanges for both halves of the wing, with a factor of safety of 1.5, is then

$$W_F = 4 \times 1.5 \frac{p}{s} \int_0^{b/2} \frac{M}{t'} dy \quad (14)$$

From equations (12) and (14), the web and the flange weights were found by graphical integration of curves of F_S and M/t' along the semispan. Values of s of 20,000 pounds per square inch for compression and 30,000 pounds per square inch for tension were used to calculate the flange weights.

In the calculation of the weight decrements due to the relieving loads, the concentrated loads shown in figure 3 were considered, and the useful loads were omitted to be conservative. The shear was assumed to be taken off at the

fuselage wall so that half the weight of the body $W_B/2$ acts at a distance y_B . The weight of the body consists of the complete weight of the fuselage and the tail, less the useful load. The nacelles and the cowling were included in the power-plant weights, W_{P_1} and W_{P_2} , and the landing-gear weight was included in W_{P_1} . The correct relative weights of the relieving loads were established by a weight analysis.

The relieving effect of each load on the web weight is proportional to the load times its distance from the center. Then, from equation (11), the web-weight decrement for both halves of the wing, with a factor of safety of 1.5 and a limit-load factor n , may be written

$$\Delta W_W = \frac{4 \times 1.5 \, pn}{s} \left(\frac{W_B}{2} y_B + W_{P_1} y_1 + W_{P_2} y_2 \right) \quad (15)$$

The same value of s was used as in the web-weight calculation.

The relieving effect of each load on the flange weight is proportional to the moment times the distance of the load from the center. Then if t_s' is 0.9 the root thickness, the weight decrement due to the relieving loads for both flanges and both halves of the wing will be, from equation (13),

$$\Delta W_F = \frac{4 \times 1.5 \, pn}{t_s' s} \left(\frac{W_B}{2} y_B^2 + W_{P_1} y_1^2 + W_{P_2} y_2^2 \right) \quad (16)$$

The same values of s were used as for the flange-weight calculation.

The final weight item W_G , which included the covering and all of the structural weight other than that of the beam, was taken as a constant proportion of the wing area. The net weights of the various structural parts of the wing and the total weights are listed in table I. As each wing weight was found, it was compared with the assumed weight used in equation (6) and the calculations were repeated until the value of the weight assumed did not affect the final weight.

RESULTS AND DISCUSSION

From the dimensions and the characteristics of the wings listed in table I, the effect of changes of the taper and of the method to prevent tip stalling may be noted. The effect of a change of the taper on $C_{L_{max}}$ and on the resulting area may be explained as follows. As the taper is increased, c_l increases from the center to the tip of the wing. In addition, the Reynolds Number decreases toward the tips so that, for the usual airfoil sections, $c_{l_{max}}$ decreases. The value of $C_{L_{max}}$ is therefore reduced and stalling tends to start nearer the tips. A greater amount of the means to prevent stalling of the tips must therefore be used to obtain the desired c_l margin, as the taper is increased. The amount required may be measured in terms of the difference, at the center of the wing, between $c_{l_{max}}$ and the c_l corresponding to $C_{L_{max}}$ (shown by Δc_l in fig. 1). Thus, Δc_l increases with taper, as listed in table I. Because of the foregoing effects, the areas also tend to increase with the taper, as shown in table I.

The change in span required to obtain the desired induced drag for the low-speed condition depends only on the value of the induced-drag factor u for wings without twist. As the value of u , which is a measure of the change of induced drag with taper for wings without twist, changes only slightly with the taper, the span varies only slightly, as shown in table I. The wings with washout, however, require a greater change in span owing to the twist, as may be seen from equation (2) and as given in the table.

The increase in area with increase in taper previously mentioned requires a reduction in thickness to obtain the required low value of the profile drag at the cruising condition. The exact value of profile drag required also depends on the induced drag at cruising speed, as the total drag must have a fixed value. This induced drag tends to be adversely affected by an increase in taper or in washout. The combined effect of washout and taper is appreciable for the wings with washout and camber increase, as shown by the values of D_i/q in the table. The foregoing effects cause the required thickness to decrease with the taper.

When the thickness was changed to make another approximation in the calculation of the characteristics of the wings, C_{Lmax} was affected as well as the drag. Whether the change increased or decreased C_{Lmax} depended on the thickness ratio near $0.7 b/2$ and on the corresponding c_{lmax} . The effect may be predicted for any particular case from figure 55 of reference 6, which shows the variation of c_{lmax} with thickness ratio. A decrease in root thickness ratio usually increased C_{Lmax} .

For the wings with camber increase, the increase in camber toward the tips increased c_{lmax} and produced higher C_{Lmax} values and lower areas. As some sharp leading edge was used for all the wings to obtain the desired c_l margin, the wings should be comparable in their avoidance of tip stalling.

For the wings with washout and camber increase, the desired margin could have been obtained by more washout but the induced drag would have been too greatly increased. Small amounts of washout were used, as listed, and the camber was increased from 3 to 4 percent of the chord as the taper ratio changed from $1/2$ to $1/3$. No further increase in camber for the wing of taper ratio $1/4$ was used because it would have produced no further increase in c_{lmax} .

With reference to the weights of the wings, it may be noted that the lowest weights were obtained for the wings with camber increase and washout. The lowest weight is indicated for a taper ratio between $1/2$ and $1/3$, as may be seen from figure 4. In order to determine whether the lowest weight had been approached, the case of taper ratio $1/3$ with washout and camber increase was investigated with twice as much washout, or 4° . The increase in washout required a reduction in thickness to obtain the desired drag at cruising speed and an increase in span to maintain the desired induced drag at low speed. The result was a considerable increase in weight.

If this analysis were applied to wings of other size, C_{Lmax} and D_0 would be affected by the change in Reynolds Number, but it is believed that considerable variation in size would be possible without altering the conclusion as to the best taper ratio. The number of engines is also of

slight importance because the effect of their relieving load on the wing weight is small. It is also believed that, for the thickness ratios in common use, the selection of a different thickness ratio for the basic wing would not appreciably alter the conclusions.

As an aid in similar calculations and to show the effect of washout on C_{D_i} , the change in C_{D_i} due to washout has been plotted in figures 5 to 7. The increase in C_{D_i} may be considered to consist of two parts, which may be found by dividing the last two terms of equation (1) by qS . The $w(\epsilon a_0)^2$ term is the increase in C_{D_i} for $C_L = 0$ and varies mainly with ϵ^2 , as w does not vary much in the usual range of taper ratios. (See fig. 6 of reference 4.) The term $v \epsilon a_0 C_L$ contributes a positive or a negative increment depending on the sign of v except that, for the elliptical wing, $v = 0$ and ΔC_{D_i} does not vary with C_L . For the tapered wings, however, ΔC_{D_i} increases with C_L for taper ratios less than about $1/2$, as may be seen from figures 5 to 7.

For taper ratios approaching 1, ΔC_{D_i} becomes negative for high values of C_L as shown by figure 7, which means that an elliptical span loading is approached owing to the washout. Values of ΔC_{D_i} for other aspect ratios and taper ratios, for either washin or washout, may be calculated from reference 4.

The values of ΔC_{D_i} given are for wings with linear twist distribution along the span. Wings are commonly constructed using straight-line elements between corresponding points of the root and the tip sections. For such a construction, the twist distribution is nonlinear and, for a given washout at the tip, ΔC_{D_i} is less than for a linear twist distribution. As an illustration of the order of magnitude of the difference that the type of twist distribution may produce, values of ΔC_{D_i} are given in figure 8 for wings with trapezoidal tips and with the two types of twist distribution. As may be seen, the differences are small. With reference to the effect of the type of twist distribution on the lift distribution, and hence on the margin against stalling of the tips, it may be said that the amount of washout required is substantially the

same for the two types of twist distribution for taper ratios between $1/3$ and 1.0 .

From the present paper and from the data given in reference 4, similar calculations can be made for wings of any size and for any aerodynamic conditions. Analyses should probably be made for wings with partial-span flaps and other high-lift devices.

CONCLUSIONS

For wings within the range of thickness ratios commonly used, designed to be aerodynamically equal, and with tip stalling avoided by the methods considered, the results of this analysis indicate that:

1. The optimum wings (the wings of the lowest weight) are obtained when tip stalling is prevented by the use of moderate washout combined with an increase in camber of the airfoil sections from the center to the tip.
2. The optimum wings have a taper ratio between $1/2$ and $1/3$.

Langley Memorial Aeronautical Laboratory,
National Advisory Committee for Aeronautics,
Langley Field, Va., May 3, 1939.

APPENDIX

Symbols

- S, wing area.
- b, span.
- b_b , span of basic wing.
- A, aspect ratio, b^2/S .
- c, chord at any section along the span.
- ϵ , aerodynamic twist, in degrees, from root to tip, measured between the zero-lift directions of the center and the tip sections, negative for washout.
- y, distance along the span measured from the center.
- y_B, y_1, y_2 , see figure 3.
- a_0 , section lift-curve slope, per degree.
- c_l , section lift coefficient; $c_l = c_{l_a} + c_{l_b}$.
- c_{l_b} , part of lift coefficient due to aerodynamic twist (computed for $C_L = 0$); $c_{l_b} = \frac{\epsilon a_0 S}{cb} L_b$.
- c_{l_a} , part of lift coefficient due to angle of attack at any C_L ; $c_{l_a} = C_L c_{l_{a1}}$.
- $c_{l_{a1}}$, part of lift coefficient due to angle of attack for $C_L = 1.0$; $c_{l_{a1}} = \frac{S}{cb} L_a$.
- L_a, L_b , additional and basic load distribution parameters. (Values of L_a and L_b were taken from reference 4 to obtain the load distributions.)
- $c_{l_{max}}$, airfoil section maximum lift coefficient.
- c_{d_0} , airfoil section profile-drag coefficient.

- C_N , wing normal-force coefficient (taken equal to C_L).
- C_L , wing lift coefficient.
- $C_{L_{max}}$, wing maximum lift coefficient.
- C_{D_0} , wing profile-drag coefficient.
- C_{D_i} , wing induced-drag coefficient.
- ΔC_{D_i} , increase in wing induced-drag coefficient due to aerodynamic twist.
- D , total wing drag.
- D_0 , wing profile drag.
- D_i , wing induced drag.
- D_{i_b} , induced drag of the basic wing.
- $u, v, \text{ and } w$, induced-drag factors (reference 4).
- n , limit-load factor.
- l , load distribution per unit length along the span.
- W_g , airplane gross weight.
- W , wing weight.
- Subscripts $W, F, \text{ and } C$ refer to web, flange, and cover weights, respectively.
- Δ refers to a weight decrement due to relieving loads.
- F_S , shear force at any point along the span.
- M , bending moment at any point along the span.
- p , specific weight (of aluminum alloy, 0.1 lb./cu. in.).
- s , allowable stress.
- t^i , effective thickness of beam at any point along span.
- t_s^i , effective thickness of beam at center of wing.

REFERENCES

1. Upson, Ralph H.: Wings - A Coordinated System of Basic Design. S.A.E. Jour., vol. XXVI, no. 1, Jan. 1930, pp. 15-30.
2. Upson, R. H., and Thompson, M. J.: The Drag of Tapered Cantilever Airfoils. Jour. Aero. Sci., vol. 1, no. 4, Oct. 1934, pp. 168-177.
3. Lachmann, G. V.: Aerodynamic and Structural Features of Tapered Wings. R.A.S. Jour., vol. XLI, no. 315, March 1937, pp. 162-212.
4. Anderson, Raymond F.: Determination of the Characteristics of Tapered Wings. T.R. No. 572, N.A.C.A., 1936.
5. Jacobs, Eastman N., Pinkerton, Robert M., and Greenberg, Harry: Tests of Related Forward-Camber Airfoils in the Variable-Density Wind Tunnel. T.R. No. 610, N.A.C.A., 1937.
6. Anderson, Raymond F.: The Experimental and Calculated Characteristics of 22 Tapered Wings. T.R. No. 627, N.A.C.A., 1938.
7. Jacobs, Eastman N., and Abbott, Ira H.: Airfoil Section Data Obtained in the N.A.C.A. Variable-Density Tunnel as Affected by Support Interference and Other Corrections. T.R. No. 669, N.A.C.A., 1939.
8. Bur. Air Commerce, U. S. Dept. Commerce: Airplane Airworthiness. Pt. 04 of Civil Air Regulations, May 1938, pp. 12 [38] and 59 [85].

TABLE I - SUMMARY OF RESULTS

Center stall obtained by -	Taper ratio	Area S (sq.ft.)	Aspect ratio, A	Span b (ft.)	Root chord, c_s (ft.)	Tip chord, c_t (ft.)	^a Root airfoil section N.A.C.A.	Tip airfoil section N.A.C.A.	Δc_l	Aerodynamic washout at tips (deg.)
Sharp leading edge	1/2	2,132	8.93	138.0	20.91	10.46	23015.4	23009	0.16	0
	1/3	2,200	8.68	138.2	24.20	8.07	23014	23009	.36	0
	1/4	2,350	8.16	138.5	27.29	6.82	23011	23009	.43	0
Washout and sharp leading edge	1/2	2,090	9.13	138.1	20.48	10.24	23015.5	23009	—	2
	1/3	2,194	8.77	138.8	23.89	7.96	23013.2	23009	—	1
Washout, camber increase, and sharp leading edge	1/2	2,082	9.15	138.0	20.40	10.20	23016	33009	—	1
	1/3	2,080	9.32	139.2	22.55	7.52	23014	43009	—	2
	1/4	2,149	9.16	140.2	24.62	6.16	23012	43009	—	2
(^a Sections with sharp leading edge.)										
Center stall obtained by -	D_o/q	D_i/q	D/q	C_L at cruising speed	Wing loading w/s	Limit-load factor, n	Weight of flanges, $W_F - \Delta W_F$ (lb.)	Weight of web, $W_W - \Delta W_W$ (lb.)	Weight of covering and bracing, W_C (lb.)	Total Weight, W (lb.)
Sharp leading edge	12.7	7.4	20.1	0.309	30.0	2.98	5,930	624	2,533	9,087
	12.8	7.4	20.2	.300	29.1	3.04	5,572	616	2,614	8,801
	12.7	7.4	20.1	.281	27.2	3.15	6,202	607	2,790	9,599
Washout and sharp leading edge	12.6	7.6	20.2	.316	30.6	2.93	5,465	582	2,481	8,528
	12.6	7.5	20.1	.300	29.2	3.03	5,656	592	2,606	8,854
Washout, camber increase, and sharp leading edge	12.7	7.4	20.1	.317	30.7	2.91	5,521	599	2,474	8,594
	12.4	7.8	20.2	.317	30.8	2.93	5,395	568	2,470	8,433
	12.3	7.9	20.2	.307	29.8	2.98	5,904	565	2,551	9,020

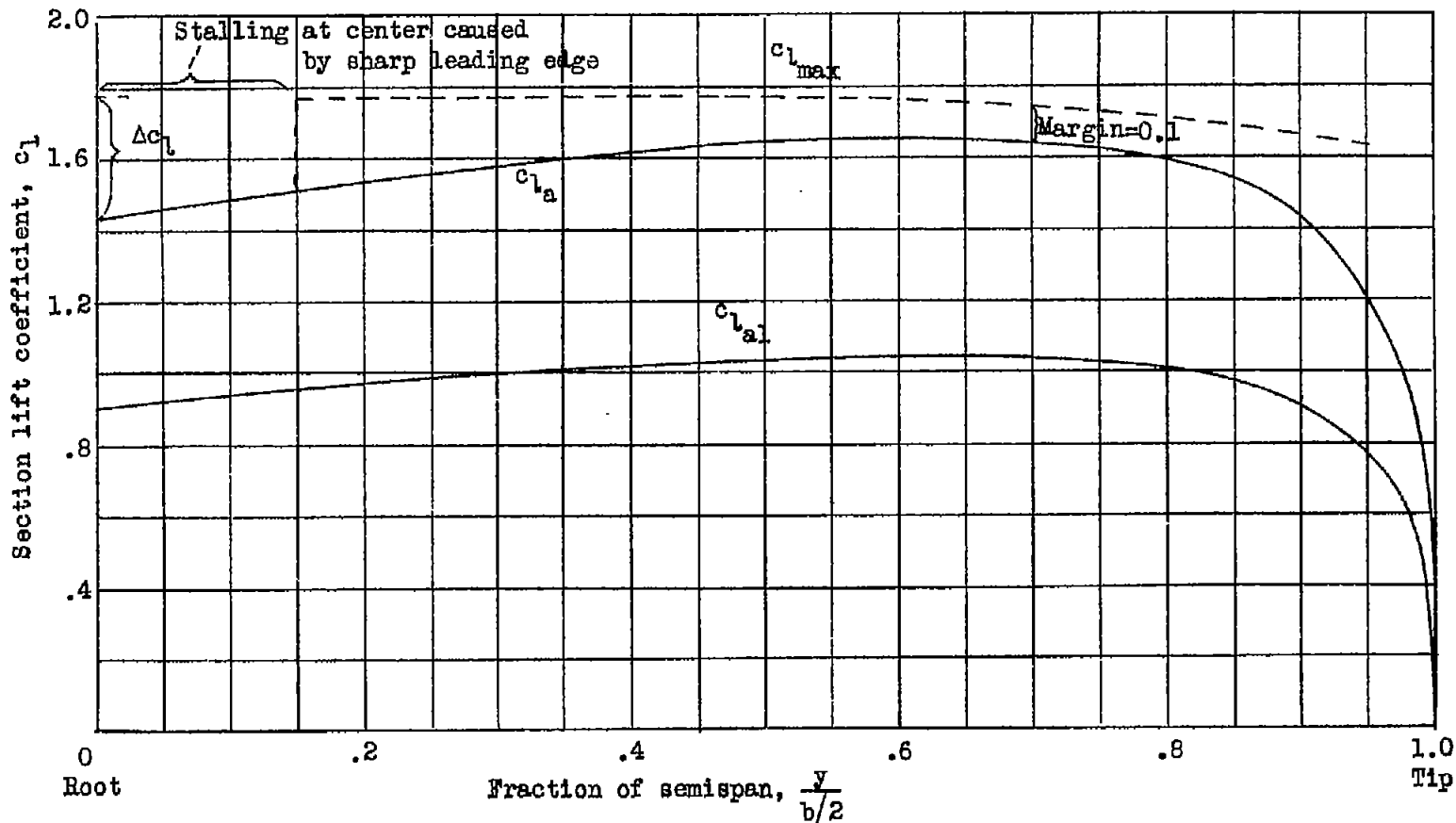
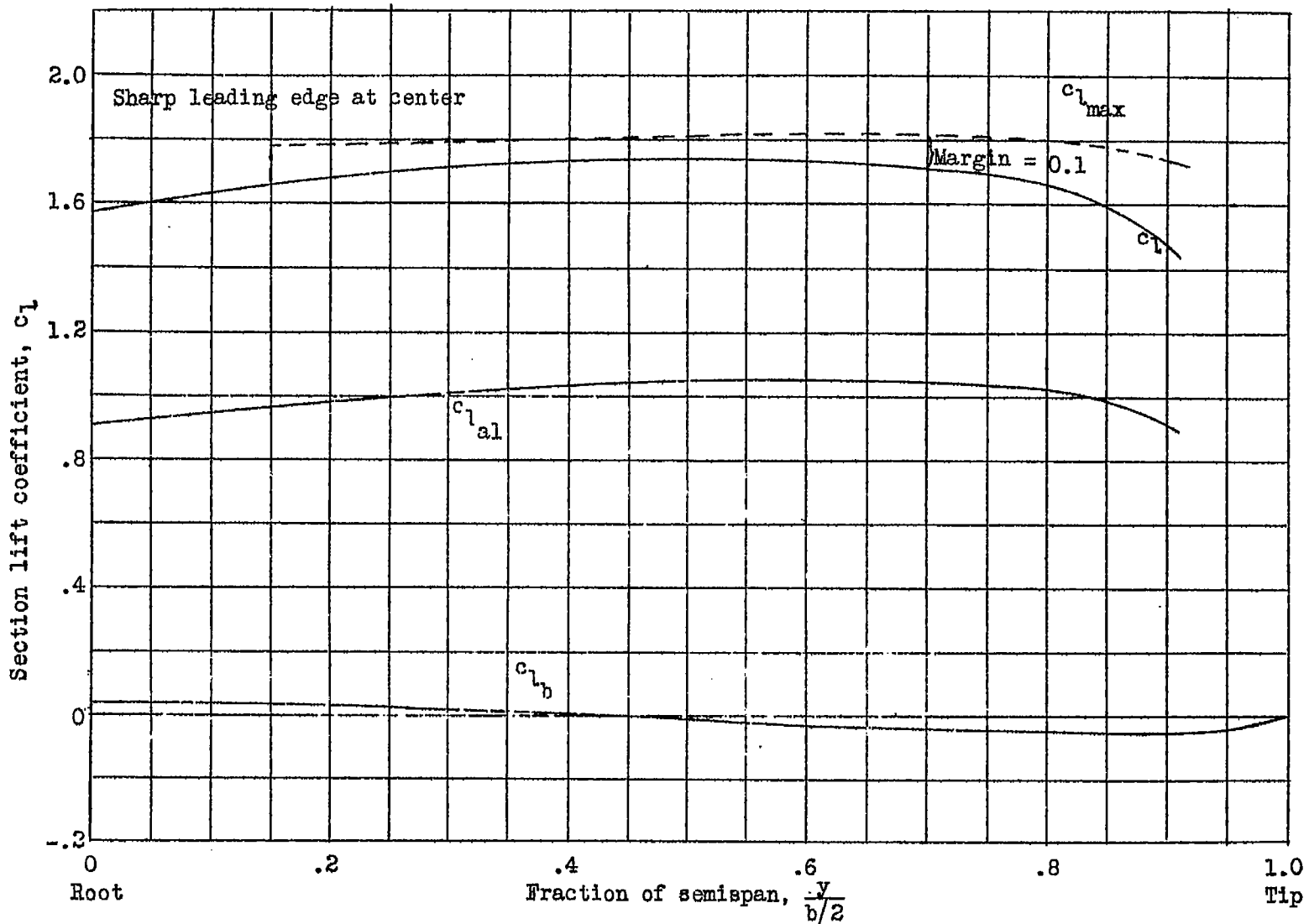


Figure 1.- Calculated stall of wing with sharp leading edge; taper-ratio, 1/3 .



N.A.C.A. Technical Note No. 713

Fig. 2

Figure 2.- Calculated stall of wing with camber increase and washout; taper ratio, 1/3.

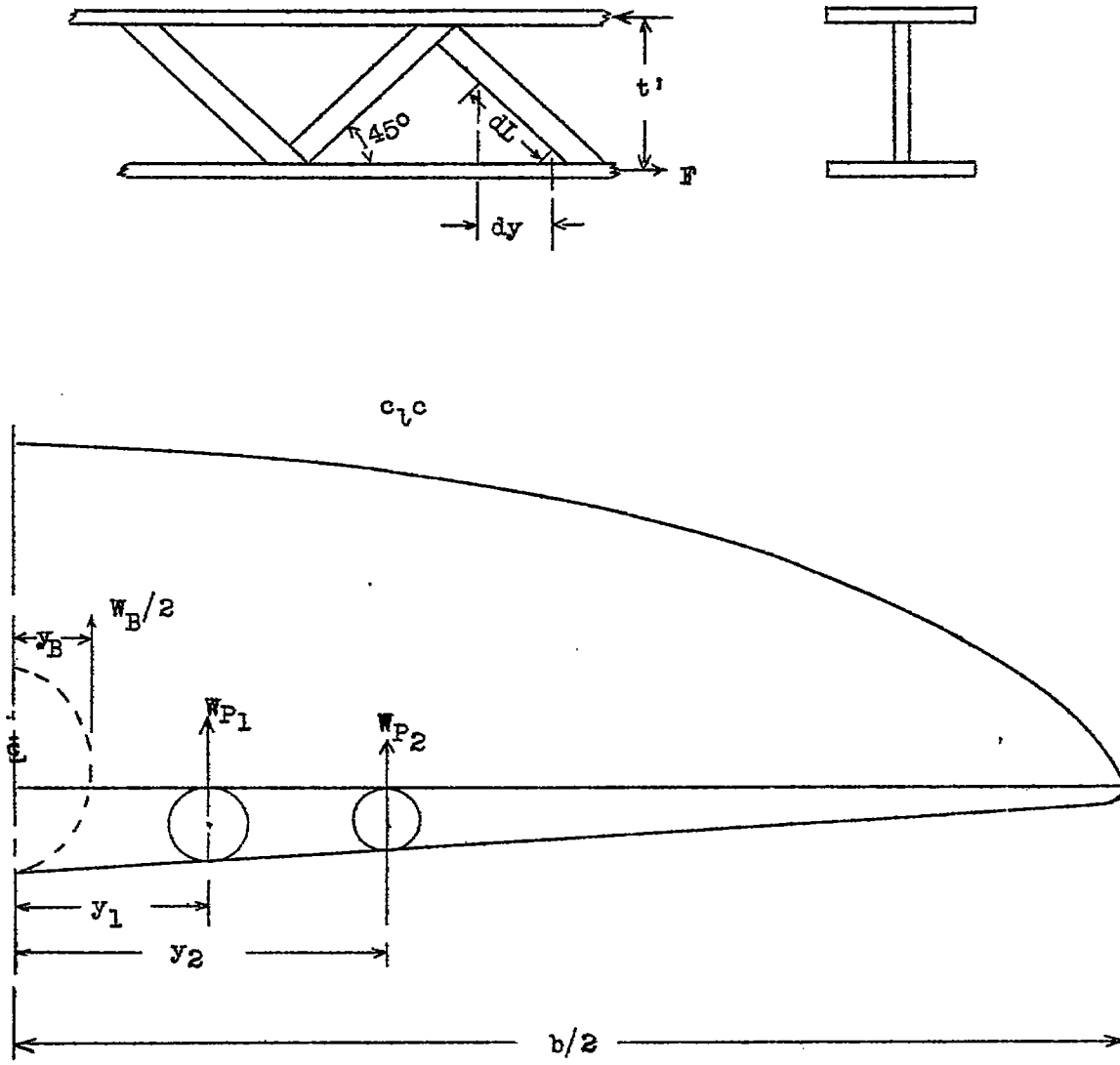


Figure 3.- Spar structure and loads on wing.

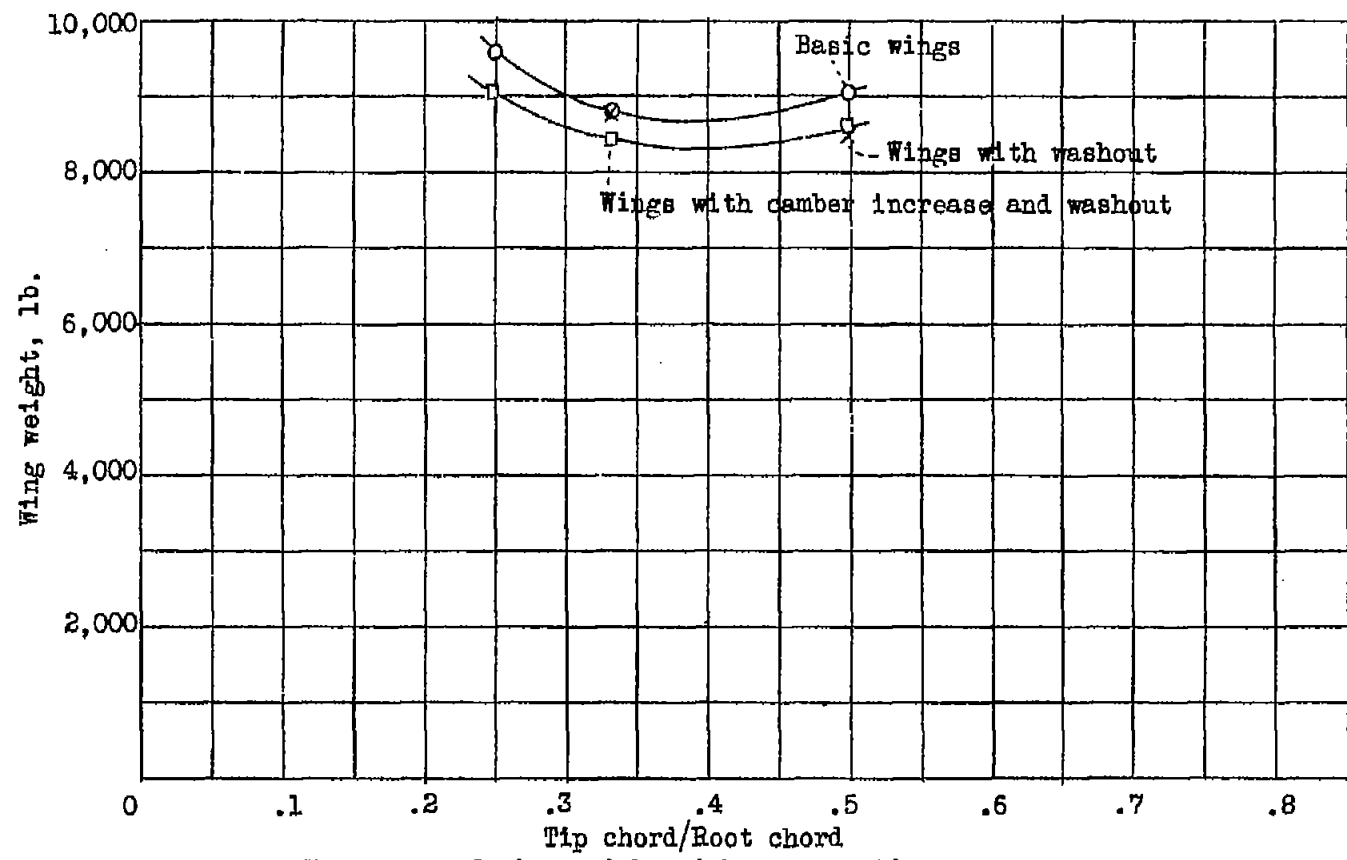


Figure 4.- Variation of wing weight with taper ratio.

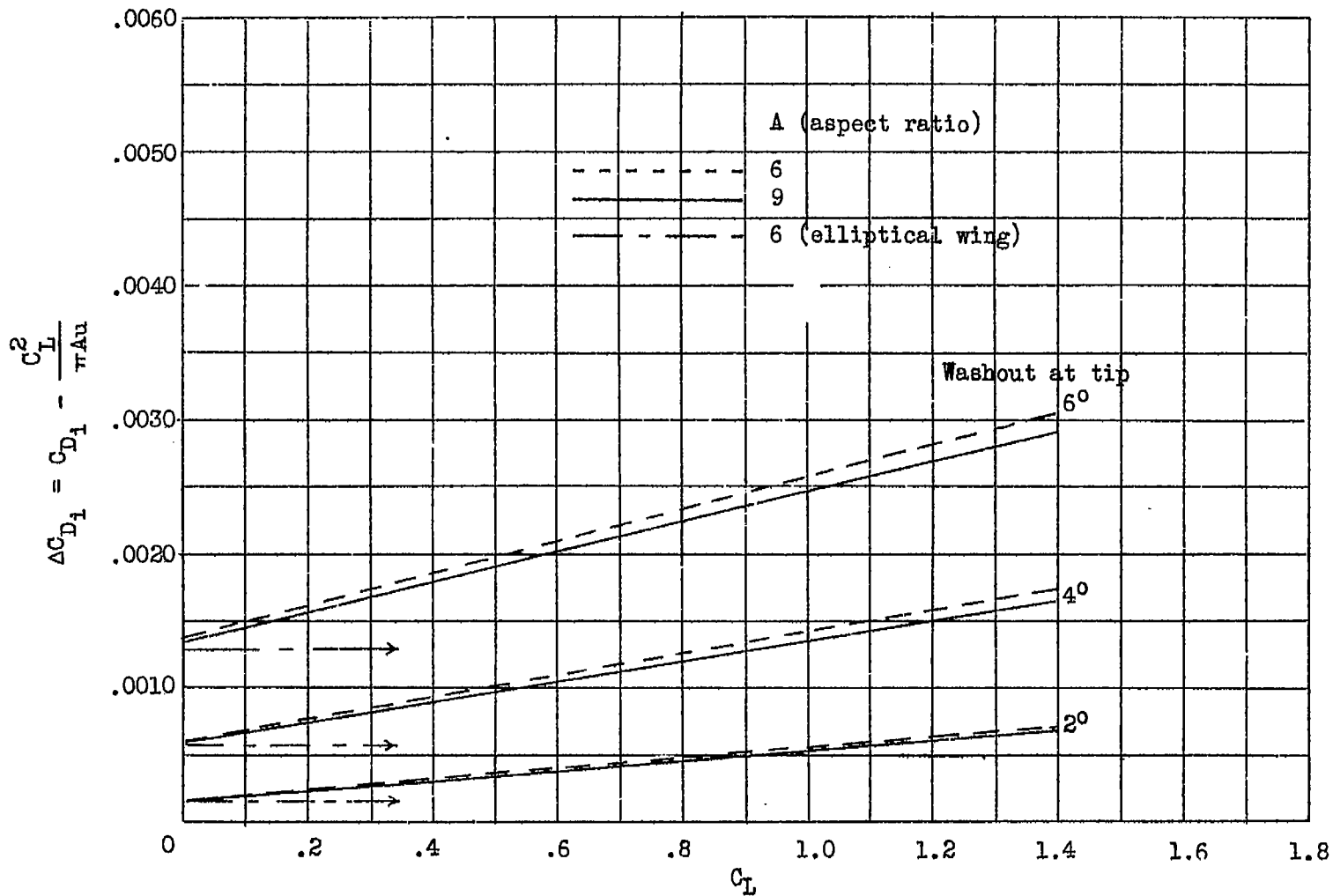


Figure 5.- Increase in induced-drag coefficient due to linear washout; rounded-tip wings; taper ratio, 1/3.

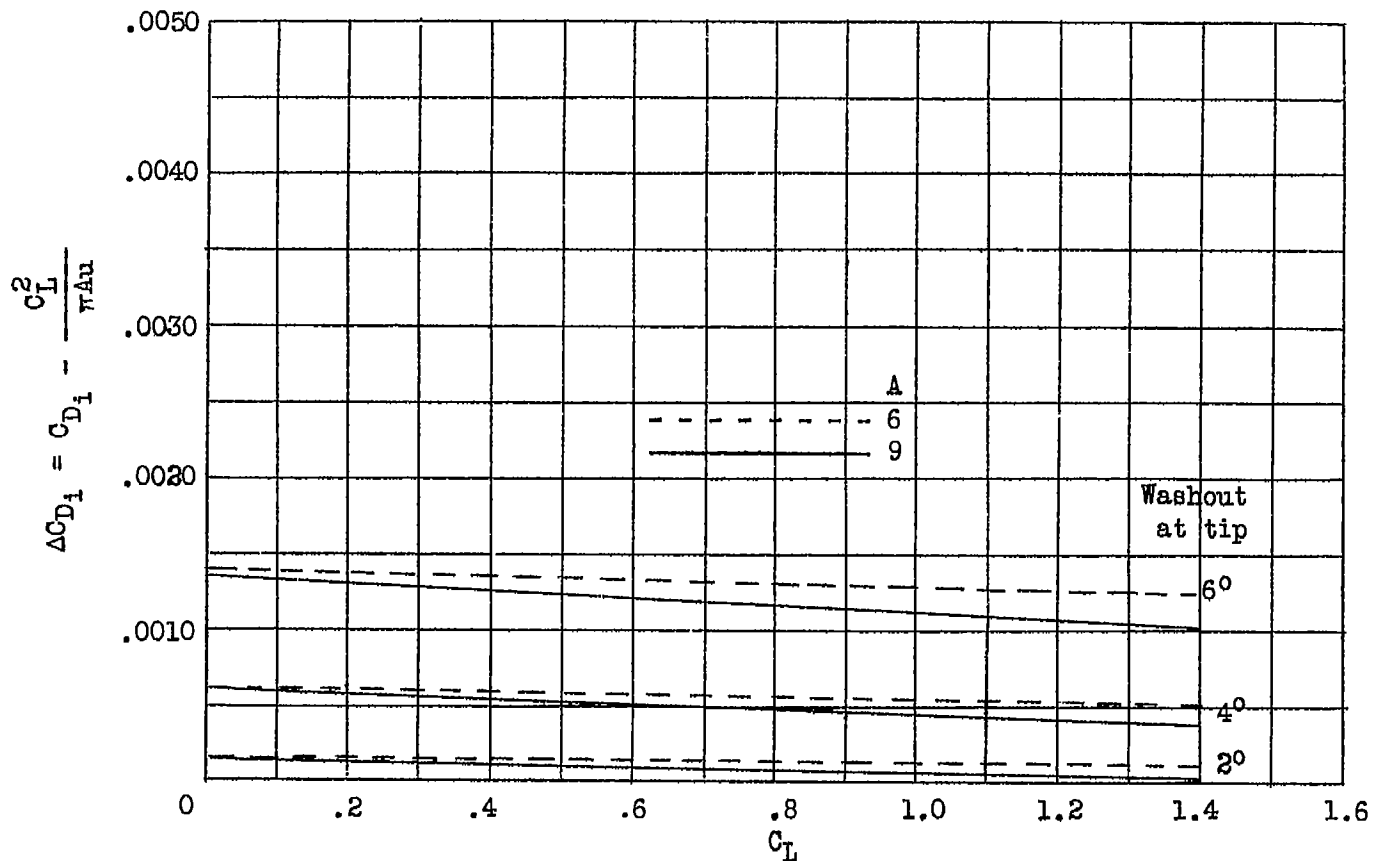


Figure 6.- Increase in induced-drag coefficient due to linear washout; rounded-tip wings; taper ratio; 1/2 .

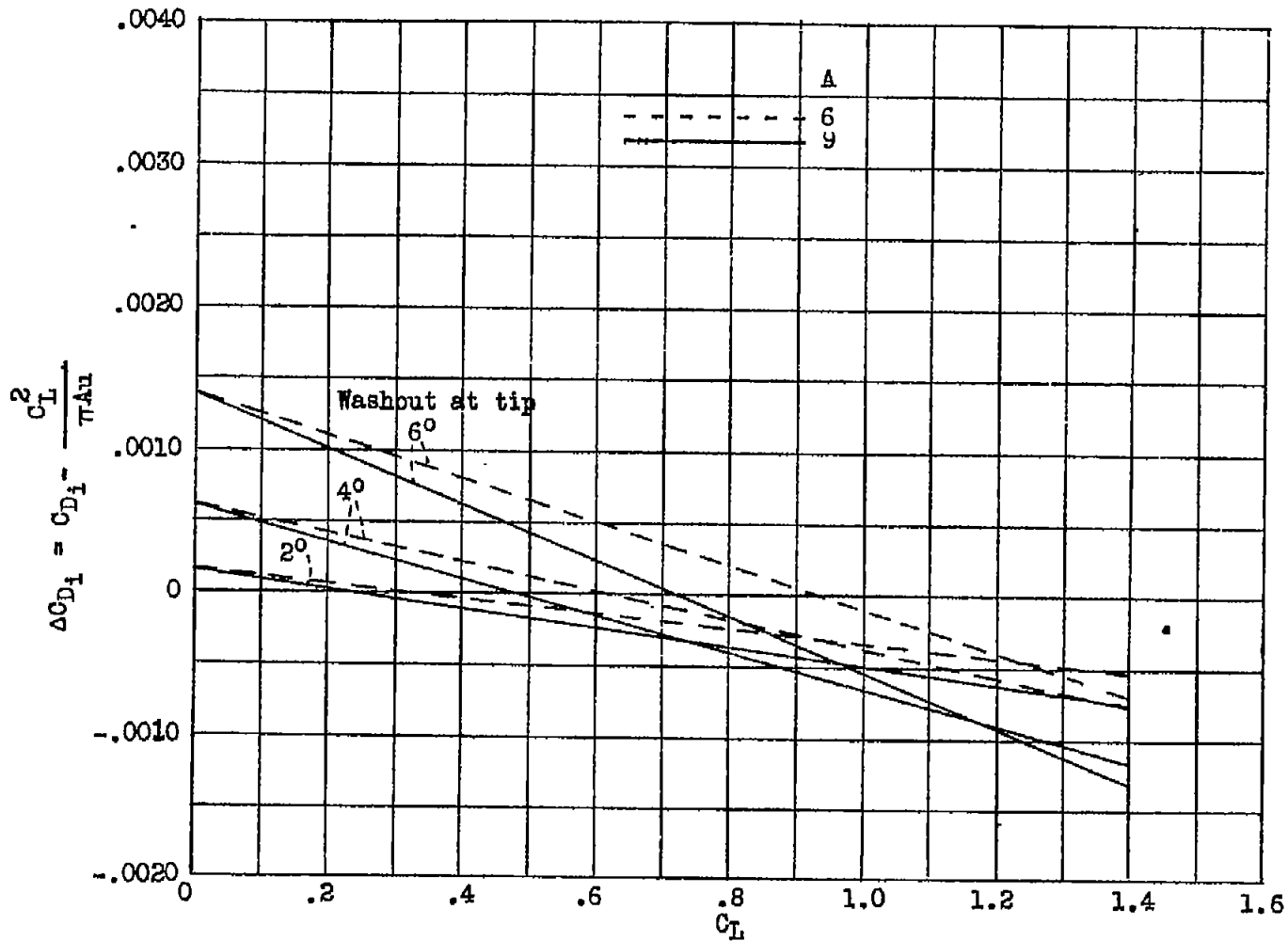


Figure 7.- Change in induced-drag coefficient due to linear washout; rounded-tip wings; taper ratio, 3/4.

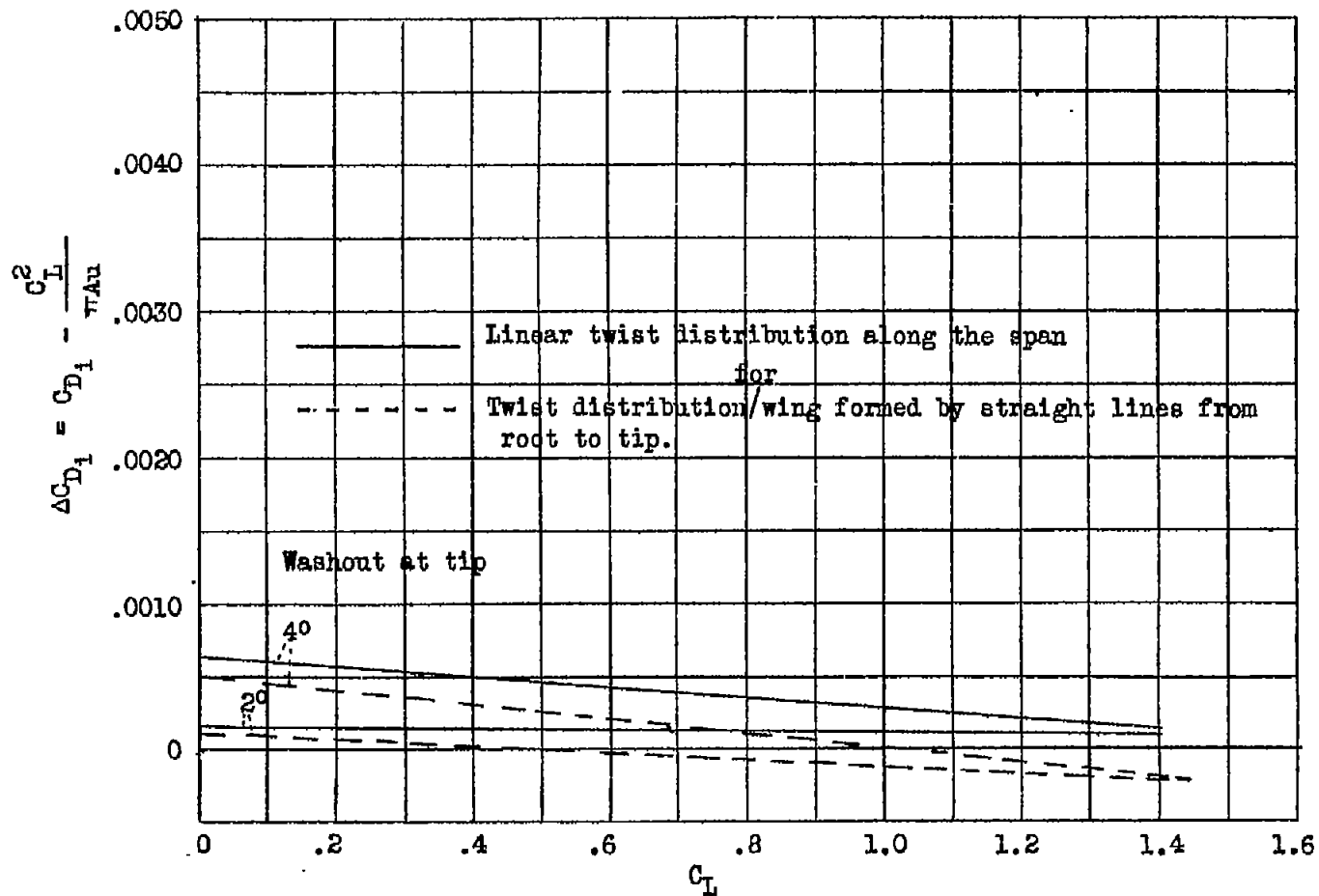


Figure 8.- Effect of type of twist distribution on ΔC_{D1} ; wings with trapezoidal tips; aspect ratio, 6 ; taper ratio, 1/2 .